

Searching for Quantum Effects in the Brain: A Bell-Type Test for Nonclassical Latent Representations in Autoencoders

I. K. Kominis,^{1,2,*} C. Xie,³ S. Li,⁴ M. Skotiniotis,^{5,6} and G. P. Tsironis^{2,7}

¹*School of Science, Zhejiang University of Science and Technology, Hangzhou 310023, China*

²*Department of Physics and Institute of Theoretical and Computational Physics, University of Crete, Heraklion 70013, Greece*

³*College of Life and Environmental Sciences, Hangzhou Normal University, Hangzhou 311121, China*

⁴*School of Automation and Electrical Engineering, Zhejiang University of Science and Technology, Hangzhou 310023, China*

⁵*Quantum Thermodynamics and Computation Group, Departamento de Electromagnetismo y Física de la Materia, Universidad de Granada, 18071 Granada, Spain*

⁶*Instituto Carlos I de Física Teórica y Computacional, Universidad de Granada, 18071 Granada, Spain*

⁷*John A. Paulson School of Engineering and Applied Sciences, Harvard University, Cambridge, MA 02138, USA*

Whether neural information processing is entirely classical or involves quantum-mechanical elements remains an open question. Here we propose a model-agnostic, information-theoretic test of nonclassicality that bypasses microscopic assumptions and instead probes the structure of neural representations themselves. Using autoencoders as a transparent model system, we introduce a Bell-type consistency test in latent space, and ask whether decoding statistics obtained under multiple readout contexts can be jointly explained by a single positive latent-variable distribution. By shifting the search for quantum-like signatures in neural systems from microscopic dynamics to experimentally testable constraints on information processing, this work opens a new route for probing the fundamental physics of neural computation.

The possibility that quantum effects play a functional role in the brain has long been a subject of debate [1]. Much of this discussion emphasized the (non)-sustainability of long-lived quantum coherence or entanglement in neural systems under physiological conditions [2, 3]. In recent years, related discussions have resurfaced [4, 5], motivated in part by growing evidence that quantum coherence can survive in biological processes, most notably in photosynthetic light harvesting and magnetoreception [6–8], and can confer functional advantages [9, 10]. These developments, together with the extreme multiscale complexity of neural systems and the persistent challenge of explaining consciousness in physical terms [11–13], have renewed interest in whether analogous mechanisms could arise in the brain [14–19]. Nonetheless, readily testable proposals remain scarce.

Here we depart from the traditional strategy of seeking quantum coherence in specific biophysical substrates. Instead, we adopt an information-theoretic perspective inspired by recent developments in machine learning [20, 21] and quantum machine learning [22–24], shifting the focus from microscopic physical realizations to the structure, efficiency, and cost of information processing itself. The extreme complexity of the brain, together with the

vast volume of information it must process under strict energetic constraints [25], strongly suggests the necessity of efficient mechanisms for compression and representation. In machine learning, autoencoders provide a standard framework for formalizing such compression, mapping high-dimensional inputs into a low-dimensional latent space from which the original inputs are reconstructed. The requirement of faithful reconstruction forces the latent variables to distill the essential structure of the input data [30]. If neural systems were to exploit quantum effects at all, it would be plausible for them to arise in encoding and compression tasks, where quantum thermodynamic resources might offer advantages to the management of information, energy and entropy bottlenecks [31, 32].

In this work we introduce a purely statistical test of nonclassicality for latent representations learned by autoencoders, and address the question: given a collection of observable reconstruction statistics obtained under different decoder settings, can *all corresponding marginals* be realized as projections of a *single positive* latent probability distribution, or is such a joint classical description impossible? Conceptually, we adopt the operational logic of Bell or contextuality tests [33–39], with decoder settings playing the role of measurement contexts and latent variables acting as hidden variables (Fig. 1). We note for completeness that there are numerous works on quantum autoencoders, which posit intrinsically

* ikominis@uoc.gr

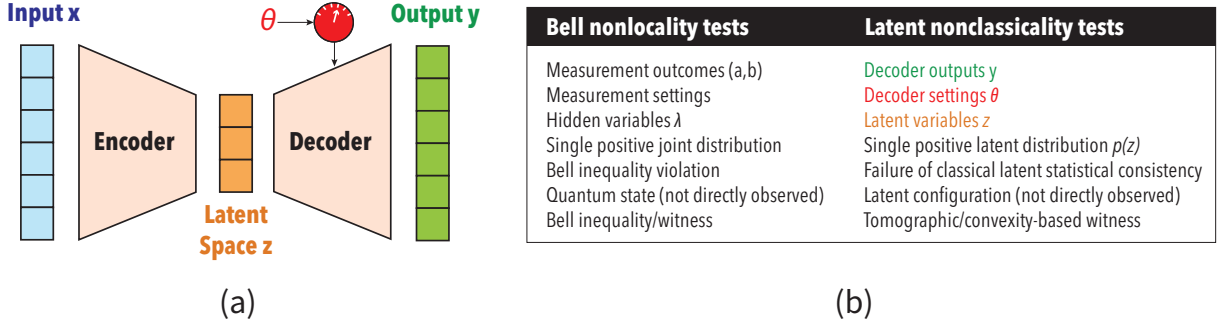


FIG. 1. (a) An autoencoder maps high-dimensional inputs x to a low-dimensional latent representation and reconstructs outputs y through multiple decoder settings θ . The latent variables are treated as unobserved degrees of freedom probed indirectly via observable decoding marginals. Nonclassicality in the latent space reflects the impossibility to account for all marginal output statistics (different decoder settings θ) with a unique positive latent distribution. (b) Analogy between Bell nonlocality tests and nonclassicality tests in the latent space of autoencoders.

quantum latent subsystems by construction [40–47]. Instead, the present work provides a Bell-type hypothesis test for the adequacy of classical latent-variable explanations themselves, entirely independent of any assumed quantum implementation.

In more detail, consider data samples x drawn from a distribution $p_{\text{data}}(x)$, an encoder $E : x \mapsto z$, and a decoder $D : z \mapsto y$. The encoder maps high-dimensional inputs x into a typically lower-dimensional latent variable z , which is intended to capture a compressed representation of the data sufficient for reconstruction. A generic autoencoder is trained to minimize a reconstruction error of the form $\mathbb{E}_x[\ell(x, D(E(x)))]$, where $\ell(x, y)$ is a loss function. While any fixed encoder E induces a conditional distribution $p(z | x)$, the reconstruction objective generally admits many distinct encoders, and hence many distinct latent representations, achieving comparable loss. As a result, the associated aggregate latent distribution, $p(z) = \int p(z | x) p_{\text{data}}(x) dx$, is not uniquely specified by the learning objective. This underdetermination motivates the question of which additional, ensemble-level restrictions on latent representations can be meaningfully imposed and, crucially, tested against observable data.

A seemingly innocuous such restriction is the assumption that all observable statistics *across readout contexts* (to be defined shortly) arise from a *single positive* latent distribution. Although this assumption appears natural and is widely taken for granted, it constitutes a foundational constraint that we here scrutinize. Concretely, in a classical latent-variable model the conditional distribution of observable outputs y , given an externally specified readout context θ , is assumed to arise from a *single positive* latent

distribution $p(z) \geq 0$, according to

$$p(y | \theta) = \int dz p(y | z, \theta) p(z) \quad (1)$$

As in contextuality tests, classicality is not a property of statistics obtained in a single context, but of their joint consistency across multiple contexts with one underlying latent distribution.

Operationally, experiments provide access to samples of the outputs y for each context θ , from which the conditional distributions $p(y | \theta)$ can be estimated. To formulate a finite-dimensional consistency test, we consider the probabilities $p(y_k | \theta_j)$ of observing outcome y_k under measurement context θ_j , with $j = 1, \dots, J$ and $k = 1, \dots, K$. The $J \times K$ array containing the probabilities $p(y_k | \theta_j)$ is concatenated (flattened) into a single vector $\mathbf{p} \in \mathbb{R}^{JK}$. Finally, the space of latent distributions is also discretized, yielding a coefficient vector $\mathbf{w} \in \mathbb{R}^N$, with $\sum_i w_i = 1$, and where N is independent of the number of measured contexts or outcomes.

The decoder induces a linear map on latent distributions, represented in the finite-dimensional setting as $\mathbf{p} = A \mathbf{w}$, where the matrix $A \in \mathbb{R}^{(JK) \times N}$ is fully determined by the decoder and the chosen set of readout settings $\{\theta_j\}$. The set of classically admissible decoding statistics forms the convex polytope $\mathcal{C} = \{A\mathbf{w} \mid \mathbf{w} \geq 0, \sum_i w_i = 1\}$. Now, we introduce a linear nonclassicality witness [49–52] as a real vector $\mathbf{c} \in \mathbb{R}^{JK}$ defining the scalar statistic $S(\mathbf{p}) = \mathbf{c} \cdot \mathbf{p}$. Also define $S_{\text{cl}} = \max_i \mathbf{c} \cdot \mathbf{a}_i$, where \mathbf{a}_i denotes the i th column of the matrix A . We observe that for any classical model $\mathbf{p} = A\mathbf{w}$, that is, when $w_i \geq 0$, it follows that $S(\mathbf{p}) = \sum_i w_i (\mathbf{c} \cdot \mathbf{a}_i) \leq (\max_i \mathbf{c} \cdot \mathbf{a}_i) \sum_i w_i = S_{\text{cl}}$. Hence, we use $\Delta(\mathbf{c}) = \mathbf{c} \cdot \mathbf{p} - S_{\text{cl}}(\mathbf{c})$ to quantify nonclassicality. Since $\Delta(\mathbf{c})$ depends on the choice of \mathbf{c} , we define

$\Delta^* = \max_{\|\mathbf{c}\|_2=1} \Delta(\mathbf{c})$. A positive value $\Delta^* > 0$ certifies nonclassicality in the ideal (noise-free) setting.

In the following, we fix a witness vector \mathbf{c} attaining (or closely approximating) the optimum Δ^* , and we model systematic degradation of the mean statistics, analogous to reduced visibility in Bell tests [57, 58]. We also include additive physical noise. If $\mathbf{p}_q \in \mathbb{R}^{JK}$ denotes the ideal decoding statistics under test, assuming an underlying nonclassicality, we define the mean observed statistics as $\mathbf{p}_\alpha = (1 - \alpha)\mathbf{p}_q + \alpha\mathbf{p}_{\text{cl}}$, where $\mathbf{p}_{\text{cl}} \in \mathcal{C}$ is a classical distribution chosen to saturate the witness bound, and $\alpha \in [0, 1]$. Thus $\alpha = 0$ corresponds to the ideal statistics, while $\alpha = 1$ yields a fully classical mean. This interpolation realizes a worst-case classical admixture that degrades the witness most rapidly and therefore provides a conservative bound on detectability.

Including additive Gaussian fluctuations, the observed statistics will be $\mathbf{p}_{\text{obs}} = \mathbf{p}_\alpha + \boldsymbol{\xi}$, where $\boldsymbol{\xi}$ is a zero-mean Gaussian noise vector with isotropic covariance $\mathbb{E}[\boldsymbol{\xi}\boldsymbol{\xi}^\top] = \sigma^2\mathbf{1}$, and $\mathbf{1}$ is the identity matrix of dimension $JK \times JK$ (formally, \mathbf{p}_{obs} is understood to be a projection of $\mathbf{p}_\alpha + \boldsymbol{\xi}$ onto the set of valid conditional distributions, enforcing non-negativity and normalization of $p(y_k \mid \theta_j)$ separately for each context θ_j). The corresponding witness value is $S_{\text{obs}} = \mathbf{c} \cdot \mathbf{p}_{\text{obs}}$, with mean $\mu_\alpha = \mathbf{c} \cdot \mathbf{p}_\alpha = (1 - \alpha)\mathbf{c} \cdot \mathbf{p}_q + \alpha S_{\text{cl}}$, and standard deviation $\sigma_S = \sigma \|\mathbf{c}\|_2$ estimated empirically from repeated trials or via bootstrap resampling [53, 54], as commonly done in finite-statistics analyses of Bell-type witnesses [55, 56]. Nonclassical structure is detected whenever $S_{\text{obs}} > S_{\text{cl}} + \kappa \sigma_S$, where e.g. $\kappa = 2$ for a one-sided 97.7% confidence level. The probability of detecting nonclassicality can be given in closed-form, $P_{\text{det}}(\alpha) = 1 - \Phi[(S_{\text{cl}} + \kappa \sigma_S - \mu_\alpha)/\sigma_S]$, where $\Phi[x] = \int_{-\infty}^x (1/\sqrt{2\pi}) e^{-t^2/2} dt$. As α increases, the mean witness value decreases linearly toward the classical bound, and $P_{\text{det}}(\alpha)$ approaches zero.

For the numerical demonstration shown in Figs. 2a,b, we use a two-dimensional latent variable (ζ, η) interrogated through a family of externally specified readout contexts θ that return linear projections $y = \zeta \cos \theta + \eta \sin \theta$. This construction is analogous to quantum homodyne tomography [59], in which quadrature measurements at different angles correspond to Radon projections of an underlying phase-space quasiprobability distribution [60]. For each readout context θ_j , the projected variable y is discretized into outcome bins $\{y_k\}$, and the corresponding probabilities $p(y_k \mid \theta_j)$ are obtained by integrating the latent distribution over the associated regions in phase space. The latent distribution is taken to be the Wigner function of the single-photon Fock state, $W_{|1\rangle}(\zeta, \eta) = \frac{2}{\pi} [4(\zeta^2 + \eta^2) - 1] \exp[-2(\zeta^2 + \eta^2)]$. The classical

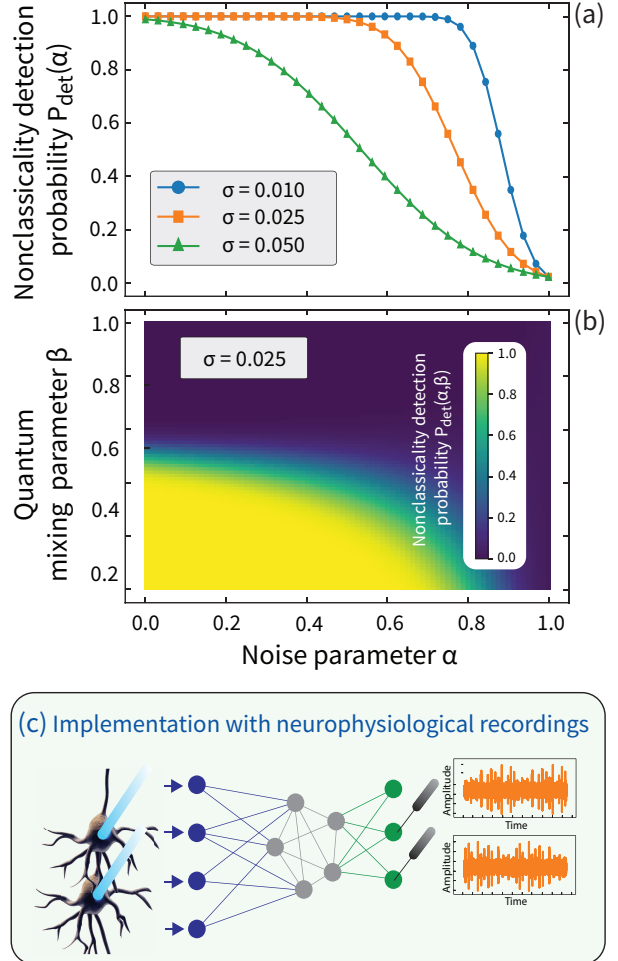


FIG. 2. (a) Nonclassicality detection probability P_{det} as a function of the noise parameter α . For the numerical implementation, a 2d latent phase space (ζ, η) is discretized on a uniform 100×100 grid over the square $[-L, L] \times [-L, L]$, with $L = 4$, yielding $N = 10^4$ latent basis points. The readout family consists of $J = 25$ projection angles $\theta_j = j\pi/J$. For each θ_j , the projected coordinate $y = \zeta \cos \theta_j + \eta \sin \theta_j$ is discretized into $K = 100$ uniformly spaced outcome bins over the interval $[-y_{\text{max}}, y_{\text{max}}]$, with $y_{\text{max}} = 1.05\sqrt{2}L$. This construction defines a forward matrix $A \in \mathbb{R}^{(JK) \times N} = \mathbb{R}^{2500 \times 10000}$. (b) The heat map again displays P_{det} , but now as a function of the noise parameter α and the quantum mixing parameter β . (c) Possible experimental realization of the proposed paradigm. Optogenetic stimulation and electrode recordings provide access to population-level activity and enable variation of decoding contexts.

consistency problem and the associated witness optimization are solved using standard Python-based convex optimization tools implemented with CVXPY. The nonclassicality detection probability is shown in Fig. 2a as a function of the mixing parameter α , for

three different values of σ .

We also assess robustness at the level of quantum states, and introduce a one-parameter family of latent quantum models with density operator $\rho_\beta = (1-\beta)|1\rangle\langle 1| + \beta\rho_{\text{th}}(1)$, where $\rho_{\text{th}}(1)$ denotes the thermal state $\rho_{\text{th}}(\bar{n}) = \sum_{n=0}^{\infty} [\bar{n}^n / (\bar{n} + 1)^{n+1}] |n\rangle\langle n|$ with mean number of photons $\bar{n} = 1$, so that the mean photon number is the same for all values of β , isolating changes in nonclassical structure from trivial variations in energy. The corresponding Wigner function is $W_{\rho_\beta} = (1 - \beta)W_{|1\rangle} + \beta W_{\text{th},1}$, where $W_{\text{th},1} = (2/3\pi) \exp[-2(\zeta^2 + \eta^2)/3]$. Now the detection probability is shown in the heat-map plot of Fig. 2b as a function of both parameters α and β , demonstrating a significant region within the quantum-classical transition and additional classical noise where detectability of nonclassicality is feasible.

To avoid the impression that our framework relies on a special physical coupling between phase-space variables and observables, we now consider an effective spin system supposed to underlie the activation of a neuron. We stress that this discussion serves only as an illustration, and no claim is made regarding the physical realization of such degrees of freedom in neural systems. Specifically, we consider a spin- j system prepared repeatedly in the same quantum state ρ_j . We will show that such a system can be mapped to the previous phase-space case. Now, each readout context θ specifies a direction \mathbf{n}_θ on the unit sphere S^2 , and the corresponding observable is the spin projection $J_{\mathbf{n}_\theta} = \mathbf{n}_\theta \cdot \mathbf{J}$, with outcomes $\in \{-j, -j+1, \dots, j\}$. Rather than resolving individual spin outcomes, we use a binary, coarse-grained readout interpreted as a neuron activation: the outcome $y = H$ (“high activation”) corresponds to spin projections exceeding a threshold, while $y = L$ (“low activation”) corresponds to projections below it. This defines a two-outcome POVM $\{E_\theta^H, E_\theta^L\}$, and the experimentally accessible statistic is the activation probability $p(\text{act} \mid \theta) = \text{Tr}(\rho_j E_\theta^{\text{act}})$, with $\text{act} = H, L$.

This construction admits a natural phase-space formulation without introducing an explicit decoder. The spin- j system possesses an SU(2) phase space given by the sphere S^2 , equipped with a Stratonovich-Weyl kernel $\Delta_j(\Omega)$, with $\Omega = (\vartheta, \varphi)$ [61]. Any state ρ defines a spherical Wigner function $W_{\rho_j}(\Omega) = \text{Tr}[\rho_j \Delta_j(\Omega)]$, while each activation POVM element admits a corresponding phase-space symbol $\Xi_\theta^{\text{act}}(\Omega) = \text{Tr}[E_\theta^{\text{act}} \Delta_j(\Omega)]$. The observed activation probabilities can therefore be written as $p(\text{act} \mid \theta) = \int d\Omega W_{\rho_j}(\Omega) \Xi_\theta^{\text{act}}(\Omega)$, which is formally identical to the latent phase-space representation introduced earlier. We note that while the formal phase-space construction applies to all spins, it is

only for $j > \frac{1}{2}$ that the outcome space and contextual incompatibility lead to meaningful restrictions on latent representations. This mirrors the fact that contextuality in the sense of Kochen–Specker arises only in Hilbert spaces of dimension three or higher [62, 63].

Interestingly, in the large- j limit, the spin- j formulation reduces locally to an effective oscillator description via the Holstein–Primakoff approximation [64], recovering the planar phase space and quadrature variables familiar from the earlier Wigner-based example. This observation is particularly relevant in quantum biophysics, where vibronic degrees of freedom are center stage, as for example in photosynthetic light-harvesting [6, 65, 66].

Although autoencoders capture general principles of efficient compression and reconstruction that are widely believed to be relevant for neural information processing, the formalism developed here does not assume that neural systems implement autoencoders or explicit latent representations. Instead, the framework is formulated entirely in terms of observable decoding statistics obtained under multiple contexts. Once abstracted from this motivating example, the proposed tests apply directly to experimental scenarios accessible with modern neural recording and control technologies (Fig. 2c). High-density electrode arrays enable simultaneous recording of large neural populations with millisecond temporal resolution, allowing decoding statistics to be estimated with high precision across repeated trials, with statistical uncertainties scaling as $1/\sqrt{M}$ in the number of trials M [67–69]. Optogenetic stimulation provides a flexible means to define and manipulate readout contexts by selectively perturbing subpopulations, modulating network states, or implementing closed-loop feedback protocols [70]. In vitro neuronal cultures and brain organoids grown on multielectrode arrays offer high-throughput platforms with precise stimulation control and long recording stability, enabling the systematic collection of large datasets across many contexts [71–73]. Assuming only statistical errors, we can connect the number of trials M with the standard deviation σ used in our numerical demonstration, noting that for roughly uniform binning with $p(y_k \mid \theta_j) \approx 1/K$ one obtains $\sigma \sim 1/\sqrt{KM}$. With the binning used in our numerical implementation ($K = 100$) and $M = 100$ trials per context, this gives $\sigma \sim 1/\sqrt{10^4} = 0.01$, matching the noise levels explored in our detection curves. Such trial numbers are achievable with the aforementioned techniques.

We note for completeness how the forward matrix A is constructed operationally. From the ensemble of observed inputs x , one defines a fixed, low-dimensional representation z , which serves solely as

an operational coordinate system for organizing the input data and carries no a priori physical interpretation. The representation space is then partitioned into a finite number N of regions $\{z_i\}$. For each readout context θ_j and each region z_i , the conditional probabilities $A_{(j,k),i} \equiv p(y_k \mid z \in z_i, \theta_j)$ are estimated empirically from repeated trials using data that are not used elsewhere in the analysis. Crucially, the representation z is not optimized to predict y , ensuring that the proposed test probes cross-context consistency of the decoding statistics rather than a trained or implicitly learned decoder.

Finally, we note that the implementation of the proposed nonclassicality test in a neurophysiological setting rests on two premises: (i) the change of measurement contexts does not affect the underlying latent (quasi)-probability distribution, and (ii) the latter is roughly stable over the measurement time.

In summary, we have introduced a model-agnostic framework for testing nonclassical statistics in neural representations, using autoencoders as a transparent motivating example. Our work shifts the search for quantum-like signatures in neural function away from microscopic mechanisms and toward robust, ensemble-level constraints on information processing. The perspective put forward in this work suggests that tools developed to test the foundations of quantum physics may also illuminate the fundamental physics of biological intelligence.

C. X. acknowledges the National Natural Science Foundation of China (grant number T235005). S. L. acknowledges the National Natural Science Foundation of China (grant number U21A20437). G.P.T. acknowledges the Department of Navy award N629092412119 issued by the Office of Naval Research Global, USA.

[1] S. Hameroff and R. Penrose, *Orchestrated reduction of quantum coherence in brain microtubules: A model for consciousness*, Math. Comp. Sim. **40**, 453 (1996).

[2] M. Tegmark, *Importance of quantum decoherence in brain processes*, Phys. Rev. E **61**, 4194 (2000).

[3] S. Hagan, S. R. Hameroff, and J. A. Tuszynski, *Quantum computation in brain microtubules: Decoherence and biological feasibility*, Phys. Rev. E **65**, 061901 (2002).

[4] B. Adams and F. Petruccione, *Quantum effects in the brain: A review*, AVS Quantum Sci. **2**, 022901 (2020).

[5] L. Gassab, O. Pusuluk, M. Cattaneo, and Ö. E. Müstecaplıoğlu, *Quantum models of consciousness from a quantum information science perspective*, Entropy **27**, 243 (2025).

[6] G. D. Scholes *et al.*, *Using coherence to enhance function in chemical and biophysical systems*, Nature **543**, 647 (2017).

[7] I. K. Kominis, *The radical-pair mechanism as a paradigm for the emerging science of quantum biology*, Mod. Phys. Lett. B **29**, 1530013 (2015).

[8] I. K. Kominis and E. Gkoudinakis, *Approaching the quantum limit of energy resolution in animal magnetoreception*, PRX Life **3**, 013004 (2025).

[9] S.F. Huelga and M.B. Plenio, *Vibrations, quanta and biology*, Contemp. Phys. **54**, 181 (2013).

[10] I. K. Kominis, *Quantum relative entropy shows singlet-triplet coherence is a resource in the radical-pair mechanism of biological magnetic sensing*, Phys. Rev. Res. **2**, 023206 (2020).

[11] M. Tegmark, *Consciousness as a state of matter*, Chaos, Solitons Fractals **76**, 238 (2015).

[12] G. Tononi, M. Boly, M. Massimini, and C. Koch, *Integrated information theory: from consciousness to its physical substrate*, Nature Rev. Neurosci. **17**, 450 (2016).

[13] N. D. Theise and J. A. Tuszynski, *Non-linearity, complexity, and quantization concepts in biology*, Front. Hum. Neurosci. **19**, 169510 (2026).

[14] M. P. A. Fisher, *Quantum cognition: The possibility of processing with nuclear spins in the brain*, Annals Phys. **362**, 593 (2015).

[15] C. Rourk, Y. Huang, M. Chen, and C. Shen, *Indication of Strongly Correlated Electron Transport and Mott Insulator in Disordered Multilayer Ferritin Structures (DMFS)*, Materials **14**, 4527 (2021).

[16] J. J. Torres and D. Manzano, *A model of interacting quantum neurons with a dynamic synapse*, New J. Phys. **24**, 073007 (2022).

[17] Z. Liu, Y.-C. Chen, and P. Ao, *Entangled biphoton generation in the myelin sheath*, Phys. Rev. E **110**, 024402 (2024).

[18] H. Neven, A. Zalcman, P. Read, K. S. Kosik, T. van der Molen, D. Bouwmeester, E. Bodnia, L. Turin, and C. Koch, *Testing the conjecture that quantum processes create conscious experience*, Entropy **26**, 460 (2024).

[19] J. J. Torres and D. Manzano, *Dissipative quantum Hopfield network: a numerical analysis*, New J. Phys. **26**, 103018 (2024).

[20] G. Carleo, I. Cirac, K. Cranmer, L. Daudet, M. Schuld, N. Tishby, L. Vogt-Maranto, and L. Zdeborová, *Machine learning and the physical sciences*, Rev. Mod. Phys. **91**, 045002 (2019).

[21] P. Mehta, M. Lukin, C.-H. Wang, A. G. R. Day, C. Richardson, C. K. Fisher, and D. J. Schwab, *A high-bias, low-variance introduction to Machine Learning for physicists*, Phys. Rep. **810**, 1 (2019).

[22] M. Schuld, I. Sinayskiy, and F. Petruccione, *An introduction to quantum machine learning*, Contemp. Phys. **56**, 172 (2015).

[23] J. Biamonte, P. Wittek, N. Pancotti, P. Rebentrost,

N. Wiebe, and S. Lloyd. *Quantum machine learning*, Nature **549**, 195 (2017).

[24] V. Dunjko and H. J. Briegel, *Machine learning & artificial intelligence in the quantum domain: a review of recent progress*, Rep. Prog. Phys. **81**, 074001 (2018).

[25] P. Lennie, *The cost of cortical computation*, Current Biol. **13**, 493 (2003).

[26] P. Baldi, *Autoencoders, unsupervised learning, and deep architectures*, in Proceedings of ICML Workshop on Unsupervised and Transfer Learning (JMLR Workshop and Conference Proceedings, 2012), pp. 37-49.

[27] Y. Bengio, A. Courville and P. Vincent, *Representation learning: A review and new perspectives*, IEEE Transactions on Pattern Analysis and Machine Intelligence **35**, 1798 (2013).

[28] U. Michelucci, *An Introduction to autoencoders*, arXiv:2201.03898.

[29] D. Bank, N. Koenigstein, and R. Giryes, *Autoencoders*, in Machine Learning for Data Science Handbook: Data Mining and Knowledge Discovery Handbook, 2023, pp. 353-74.

[30] N. Tishby and N. Zaslavsky, *Deep learning and the information bottleneck principle*, 2015 IEEE Information Theory Workshop (ITW), Jerusalem, Israel, 2015, pp. 1-5

[31] J. M. R. Parrondo, J. M. Horowitz, and T. Sagawa, *Thermodynamics of information*, Nat. Phys. **11**, 131 (2015).

[32] S. Vinjanampathy and J. Anders, *Quantum thermodynamics*, Contemp. Phys. **57**, 545 (2016).

[33] R. W. Spekkens, *Negativity and contextuality are equivalent notions of nonclassicality*, Phys. Rev. Lett. **101**, 020401 (2008).

[34] A. Cabello, *Experimentally testable state-independent quantum contextuality*, Phys. Rev. Lett. **101**, 210401 (2008).

[35] R. Horodecki, P. Horodecki, M. Horodecki, and K. Horodecki, *Quantum entanglement*, Rev. Mod. Phys. **81**, 865 (2009).

[36] N. Brunner, D. Cavalcanti, S. Pironio, V. Scarani, and S. Wehner, *Bell nonlocality*, Rev. Mod. Phys. **86**, 419 (2014).

[37] L. K. Shalm *et al.*, *Strong loophole-free test of local realism*, Phys. Rev. Lett. **115**, 250402 (2015).

[38] D. Cavalcanti and P. Skrzypczyk, *Quantum steering: a review with focus on semidefinite programming*, Rep. Prog. Phys. **80**, 024001 (2017).

[39] C. Budroni, A. Cabello, O. Ghne, M. Kleinmann, and J.-A. Larsson, *Kochen-Specker contextuality*, Rev. Mod. Phys. **94**, 045007 (2022).

[40] J. Romero, J. P. Olson, and A. Aspuru-Guzik, *Quantum autoencoders for efficient compression of quantum data*, Quantum Sci. Technol. **2**, 045001 (2017).

[41] C. Bravo-Prieto, *Quantum autoencoders with enhanced data encoding*, Mach. Learn.: Sci. Technol. **2**, 035028 (2021).

[42] A. Sakhnenko, C. O'Meara, K. J. B. Ghosh, C. B. Mendl, G. Cortiana, and J. Bernab  -Moreno, *Hybrid classical-quantum autoencoder for anomaly detection*, Quantum Mach. Intell. **4**, 27 (2022).

[43] D. F. Locher, L. Cardarelli, and M. M  ller, *Quantum error correction with quantum autoencoders*, Quantum **7**, 942 (2023).

[44] A. Chalkiadakis, M. Theocharakis, G. D. Bamparis, and G. P. Tsironis, *Quantum neural networks for the discovery and implementation of quantum error-correcting codes*, Chaos **33**, 113127 (2023).

[45] H. Ma, C.-J. Huang, C. Chen, D. Dong, Y. Wang, R.-B. Wu, G.-Y. Xiang, *On compression rate of quantum autoencoders: Control design, numerical and experimental realization*, Automatica **147**, 110659 (2023).

[46] J. Wu, H. Fu, M. Zhu, H. Zhang, W. Xie and X.-Y. Li, *Quantum circuit autoencoder*, Phys. Rev. A **109**, 032623 (2024).

[47] , R. Frehner and K. Stockinger, *Applying quantum autoencoders for time series anomaly detection*, Quantum Mach. Intell. **7**, 59 (2025).

[48] A. Makhzani, J. Shlens, N. Jaitly, I. Goodfellow, and B. Frey, *Adversarial autoencoders*, arXiv:1511.05644.

[49] B. Morris, L. J. Fiderer, B. Lang, and D. Goldwater, *Witnessing Bell violations through probabilistic negativity*, Phys. Rev. A **105**, 032202 (2022).

[50] A. C. B. Greenwood, L. T. H. Wu, E. Y. Zhu, B. T. Kirby, and L. Qian, *Machine-learning-derived entanglement witnesses*, Phys. Rev. Appl. **19**, 034058 (2023).

[51] V. Gulati, G. Singh, and K. Dorai, *Using linear and nonlinear entanglement witnesses to generate and detect bound entangled states on an IBM quantum processor*, Phys. Scr. **99**, 115122 (2024).

[52] S. Boyd and L. Vandenberghe, *Convex Optimization* (Cambridge University Press, Cambridge, 2004).

[53] B. Efron, *Bootstrap methods: Another look at the jackknife*, Ann. Statist. **7**, 1 (1979).

[54] B. Efron and R. J. Tibshirani, *An Introduction to the Bootstrap* (Chapman & Hall/CRC, New York, 1994).

[55] J.-Å. Larsson, *Bell's inequality and detector inefficiency*, Phys. Rev. A **57**, 3304 (1998).

[56] R. D. Gill, *Statistics, causality and Bell's theorem*, Statist. Sci. **29**, 512 (2014).

[57] P. G. Kwiat, A. M. Steinberg, and R. Y. Chiao, *High-visibility interference in a Bell-inequality experiment for energy and time*, Phys. Rev. A **47**, R2472 (1993).

[58] M. Tomasin, E. Mantoan, J. Jogenfors, G. Vallone, J.-A. Larsson, and Paolo Villoresi, *High-visibility time-bin entanglement for testing chained Bell inequalities*, Phys. Rev. A **95**, 032107 (2017).

[59] A. I. Lvovsky and M. G. Raymer, *Continuous-variable optical quantum-state tomography*, Rev. Mod. Phys. **81**, 299 (2009).

[60] W. P. Schleich, *Quantum optics in phase space* (Wiley-VCH Verlag, Berlin 2001).

[61] R. P. Rundle and M. J. Everitt, *Overview of the phase space formulation of quantum mechanics with application to quantum technologies*, Adv. Quantum

Technol. **4**, 2100016 (2021).

[62] A. M. Gleason, *Measures on the closed subspaces of a Hilbert space*, J. Math. Mech. **6**, 885 (1957).

[63] S. Kochen and E. P. Specker, *The problem of hidden variables in quantum mechanics*, J. Math. Mech. **17**, 59 (1967).

[64] K. Hammerer, A. S. Sørensen, and E. S. Polzik, *Quantum interface between light and atomic ensembles*, Rev. Mod. Phys. **82**, 1041 (2010).

[65] A. Ishizaki and G. R. Fleming, *Theoretical examination of quantum coherence in a photosynthetic system at physiological temperature*, Proc. Natl. Acad. Sci. U.S.A. **106**, 17255 (2009).

[66] J. Cao *et al.*, *Quantum biology revisited*, Sci. Adv. **6**, eaaz4888 (2020).

[67] B. B. Averbeck, P. E. Latham, and A. Pouget, *Neural correlations, population coding and computation*, Nat. Rev. Neurosci. **7**, 358 (2006).

[68] L. Paninski, J. Pillow, and J. Lewi, *Statistical models for neural encoding, decoding, and optimal stimulus design*, Prog. Brain Res. **165**, 493 (2007).

[69] I. H. Stevenson and K. P. Kording, *How advances in neural recording affect data analysis*, Nat. Neurosci. **14**, 139 (2011).

[70] L. Grosenick, J. H. Marshel, and K. Deisseroth, *Closed-loop and activity-guided optogenetic control*, Neuron **86**, 106 (2015).

[71] J. J. Jun *et al.*, *Fully integrated silicon probes for high-density recording of neural activity*, Nature **551**, 232 (2017).

[72] C. A. Trujillo *et al.*, *Complex oscillatory waves emerging from cortical organoids*, Nat. Neurosci. **22**, 166–174 (2019).

[73] T. Sharf *et al.*, *Functional neuronal circuitry and oscillatory dynamics in human brain organoids*, Nat. Comm. **13**, 4403 (2022).

[74] M. E. J. Obien, K. Deligkaris, T. Bullmann, D. J. Bakkum, and U. Frey, *Revealing neuronal function through microelectrode array recordings*, Front. Neurosci. **8**, 423 (2015).

[75] C. A. Trujillo *et al.*, *Complex oscillatory waves emerging from cortical organoids model early human brain network development*, Cell Stem Cell **25**, 558 (2019).

[76] A. M. Packer, L. E. Russell, H. W. P. Dagleish, and M. Häusser, *Simultaneous all-optical manipulation and recording of neural circuit activity with cellular resolution in vivo*, Nat. Methods **12**, 140 (2015).

[77] C. Stringer, M. Pachitariu, N. Steinmetz, C. Reddy, M. Carandini, and K. D. Harris, *High-dimensional geometry of population responses in visual cortex*, Nature **571**, 361 (2019).